Part 2b. Viral infection and immune response

Virus replication

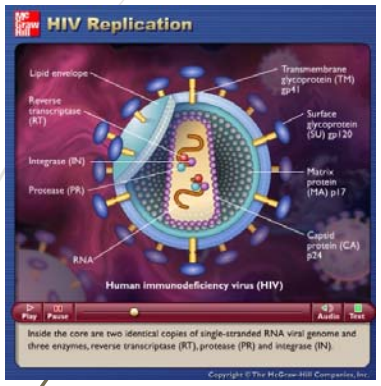

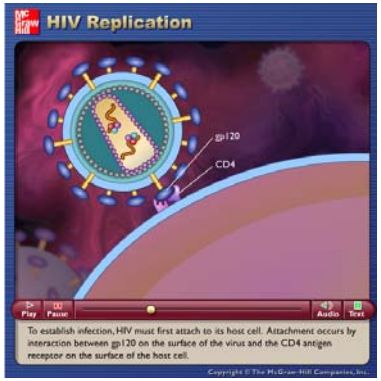

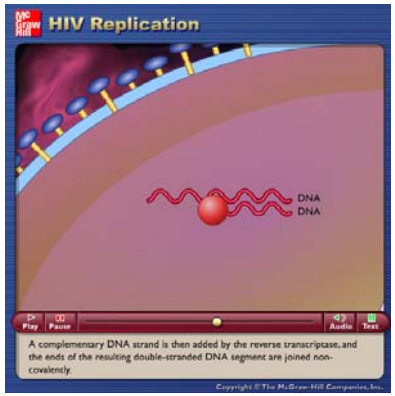

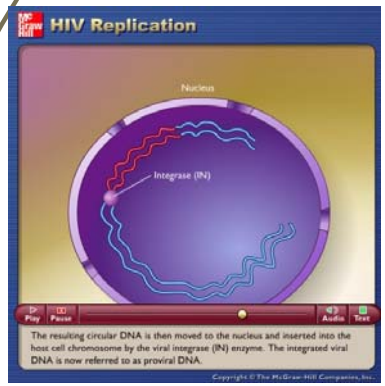

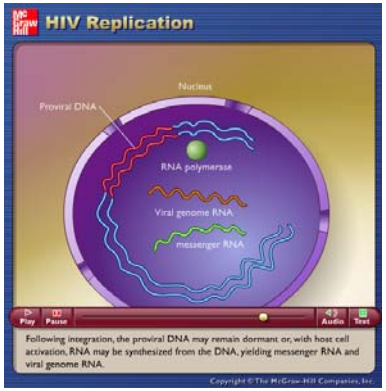

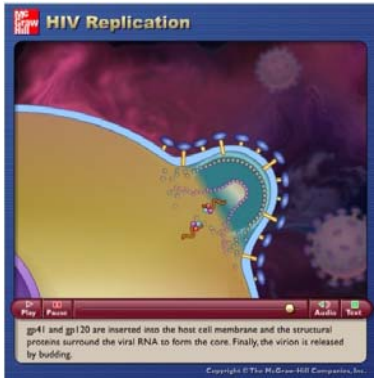

Innate and adaptive immune response

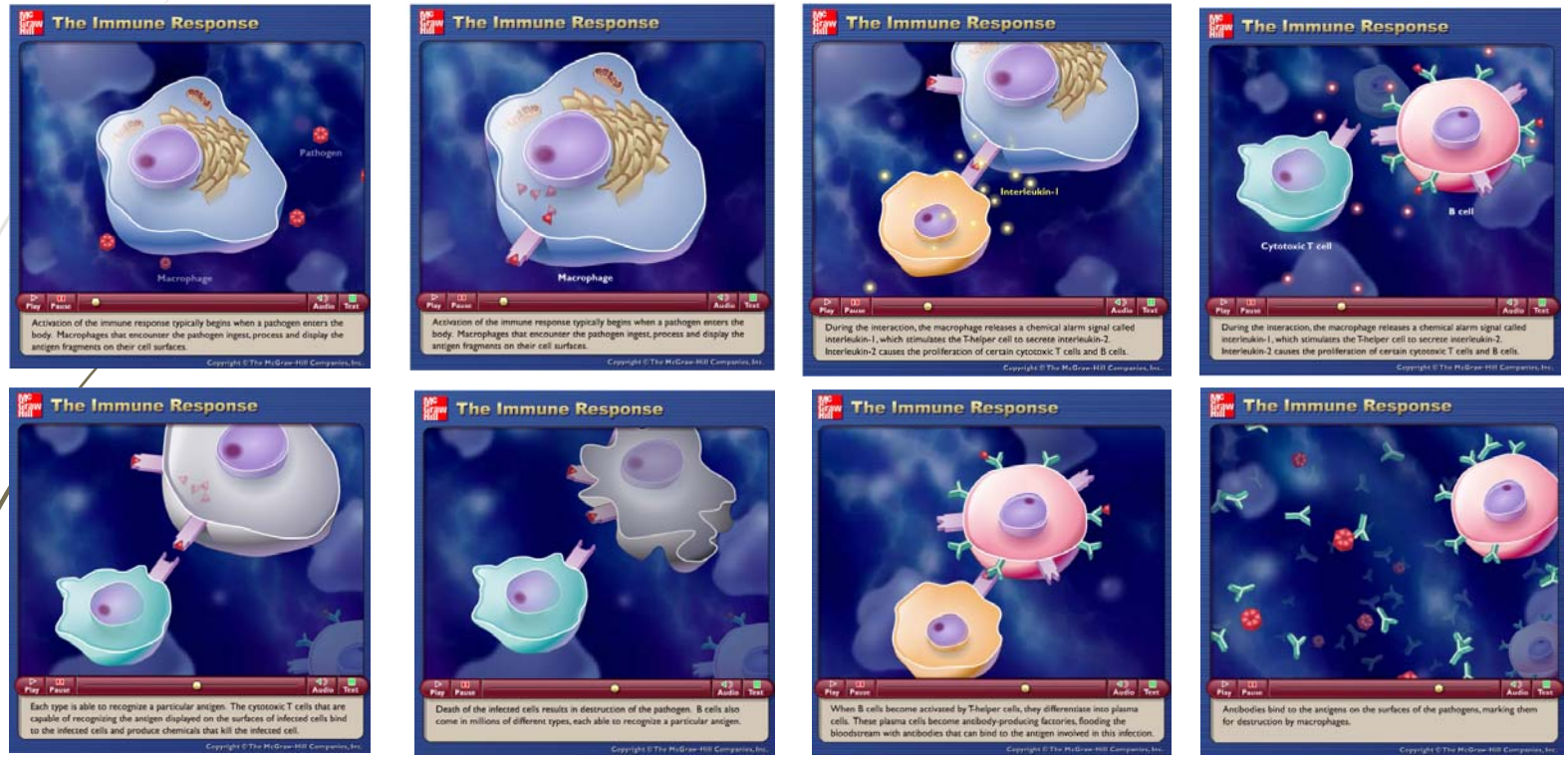

http://highered.mheducation.com/sites/0072495855/student_view0/chapter24/animation__the_immune_response.html

Virus multiplication assays (cell culture)

Detecting viruses: the plaque assay

6 July 2009 by Vincent Racaniello

One of the most important procedures in virology is measuring the virus titer – the concentration of viruses in a sample. A widely used approach for determining the quantity of infectious virus is the plaque assay. This technique was first developed to calculate the titers of bacteriophage stocks. Renato Dulbecco modified this procedure in 1952 for use in animal virology, and it has since been used for reliable determination of the titers of many different viruses.

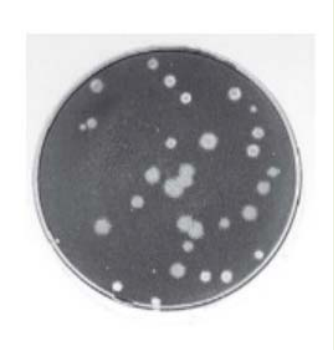

example shown below, there are 17 plaques on the plate made from the 10^{-6} dilution. The titer of the virus stock is therefore 1.7×10^{8} PFU/ml.

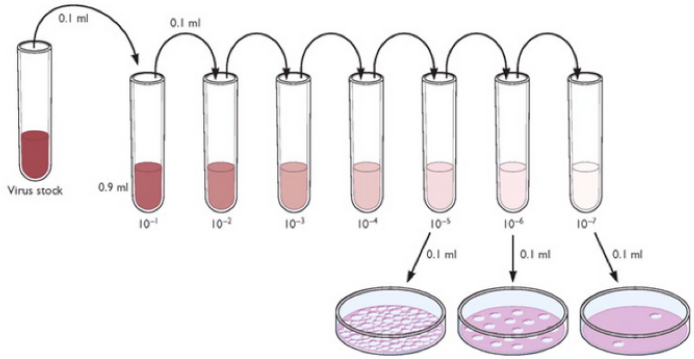

https://www.virology.ws/2009/07/06/detecting-viruses-the-plaque-assay/

Viral infection in cell culture

$$\frac{\partial U}{\partial t} = -aUV,$$

Uninfected cells

$$\frac{\partial I}{\partial t} = aUV - \beta I,$$

Infected cells

$$\frac{\partial V}{\partial t} = D\frac{\partial^2 V}{\partial x^2} + bI_\tau - \sigma V$$

Virus

$$I_\tau(x) = I(x, t - \tau)$$

Reduction

$$\frac{\partial U}{\partial t} = -aUV,$$

$$\frac{\partial I}{\partial t} = aUV - \beta I,$$

$$\frac{\partial V}{\partial t} = D\frac{\partial^2 V}{\partial x^2} + bI_\tau - \sigma V$$

Beta=0

$$U + I = w_0$$

$$\frac{\partial I}{\partial t} = a(w_0 - I)V,$$

$$\frac{\partial V}{\partial t} = D\frac{\partial^2 V}{\partial x^2} + bI_\tau - \sigma V.$$

Monotone system with time delay

Example of simulations

$$\frac{\partial I}{\partial t} = a(w_0 - I)V,$$

$$\frac{\partial V}{\partial t} = D\frac{\partial^2 V}{\partial x^2} + bI_\tau - \sigma V.$$

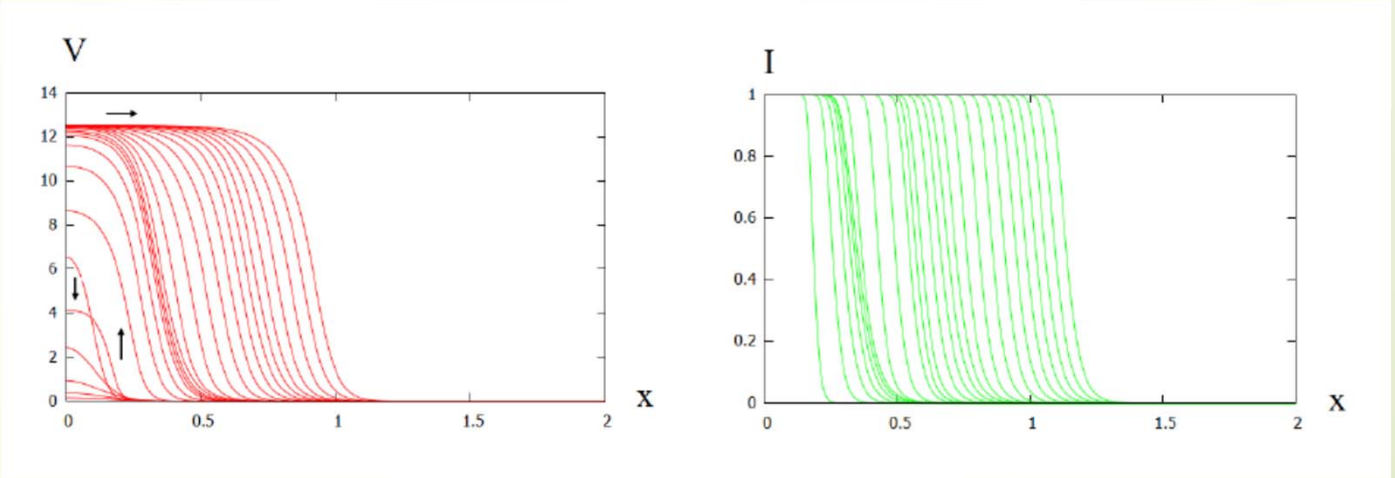

Waves

$$\frac{\partial I}{\partial t} = a(w_0 - I)V,$$

$$\frac{\partial V}{\partial t} = D\frac{\partial^2 V}{\partial x^2} + bI_\tau - \sigma V.$$

$$I(x,t) = w(x - ct), \quad V(x,t) = v(x - ct).$$

$$cw' + a(w_0 - w)v = 0,$$

$$Dv'' + cv' + bw(\xi + c\tau) - \sigma v = 0$$

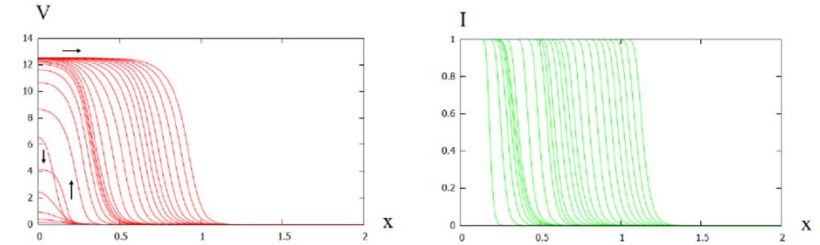

$$w(\infty) = v(\infty) = 0\,, \quad w(-\infty) = w_0\,, \quad v(-\infty) = \frac{bw_0}{\sigma}$$

Minimal wave speed: method of linearization

$$cw' + a(w_0 - w)v = 0,$$

$$Dv'' + cv' + bw(\xi + c\tau) - \sigma v = 0$$

$\tau = 0:\ \mu = 4.57,\ F(\mu) = 0.00618,\ c = 0.077$ (numerical value 0.075),

$\tau = 1:\ \mu = 1.89,\ F(\mu) = 0.00171,\ c = 0.041$ (numerical value 0.039),

$\tau = 2:\ \mu = 1.29,\ F(\mu) = 0.00098,\ c = 0.031$ (numerical value 0.029).

Linearizing system (1.6), (1.7) at ∞, we obtain the system

$$cw' + aw_0 v = 0, \tag{3.1}$$

$$Dv'' + cv' + bw(\xi + c\tau) - \sigma v = 0. \tag{3.2}$$

We look for the solution in the form

$$w(\xi) = pe^{-\lambda\xi}, \quad v(\xi) = qe^{-\lambda\xi}.$$

Then

$$-cp\lambda + aw_0 q = 0, \tag{3.3}$$

$$Dq\lambda^2 - cq\lambda + bpe^{-\lambda c\tau} - \sigma q = 0. \tag{3.4}$$

We express p from equation (3.3) and substitute in equation (3.4):

$$(D\lambda^2 - c\lambda - \sigma)c\lambda e^{\lambda c\tau} = -abw_0. \tag{3.5}$$

Set $\mu = c\lambda$. Then

$$\left(D\frac{\mu^2}{c^2} - \mu - \sigma\right)\mu e^{\mu\tau} = -abw_0$$

and, hence,

$$c^2 = \frac{D\mu^3 e^{\mu\tau}}{\mu(\mu + \sigma)e^{\mu\tau} - abw_0} \equiv F(\mu).$$

There exits $c_0 > 0$ such that this equation has two solutions μ for any $c > c_0$. The minimal wave speed c_0 is given by the equality

$$c_0^2 = \min_{\mu > 0} \frac{D\mu^3 e^{\mu\tau}}{\mu(\mu + \sigma)e^{\mu\tau} - abw_0}. \tag{3.6}$$

Wave existence: method of upper and lower functions

$$cw' + aw_0 v = 0,$$

$$Dv'' + cv' + bw(\xi + c\tau) - \sigma v = 0.$$

Theorem.

Waves exist for c greater than or equal to c_0 if time delay tau is less than some tau_0

SARS-CoV in the culture of epithelial (cilia) cells

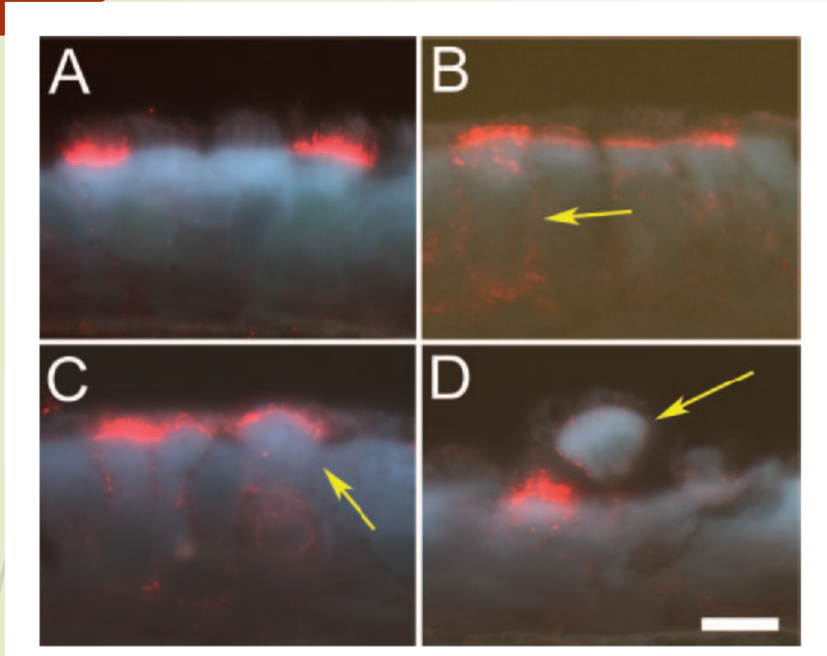

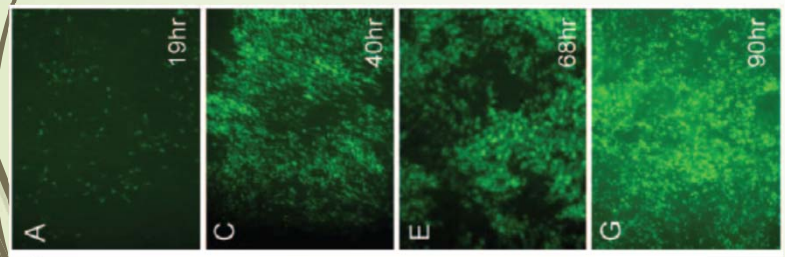

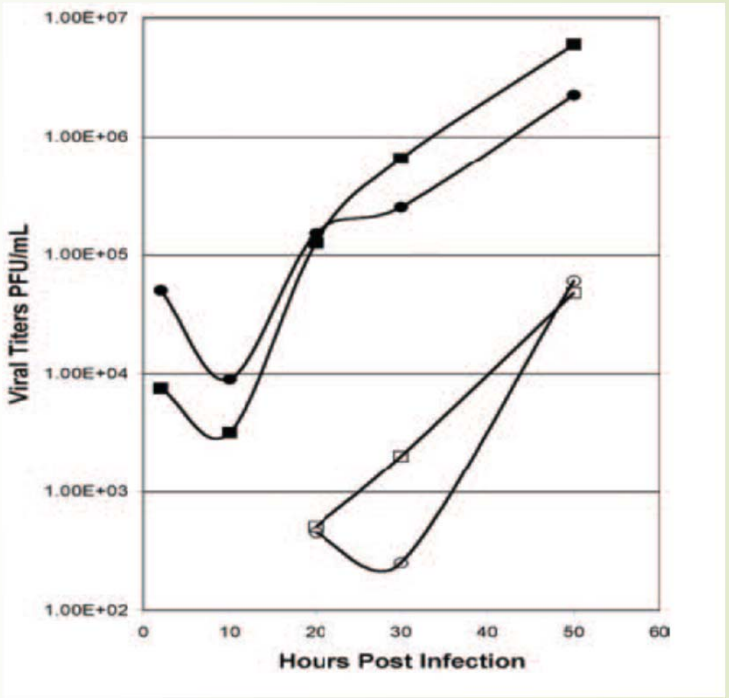

JOURNAL OF VIROLOGY, Dec. 2005, p. 15511–15524 Vol. 79, No. 24
0022-538X/05/$08.00+0 doi:10.1128/JVI.79.24.15511–15524.2005

Severe Acute Respiratory Syndrome Coronavirus Infection of Human Ciliated Airway Epithelia: Role of Ciliated Cells in Viral Spread in the Conducting Airways of the Lungs

Amy C. Sims,[1*] Ralph S. Baric,[1,2] Boyd Yount,[1] Susan E. Burkett,[3] Peter L. Collins,[4] and Raymond J. Pickles[2,3]

Comparison with experiments

$$V_T(t) = \int_0^L V(x,t)dx$$

Total viral load

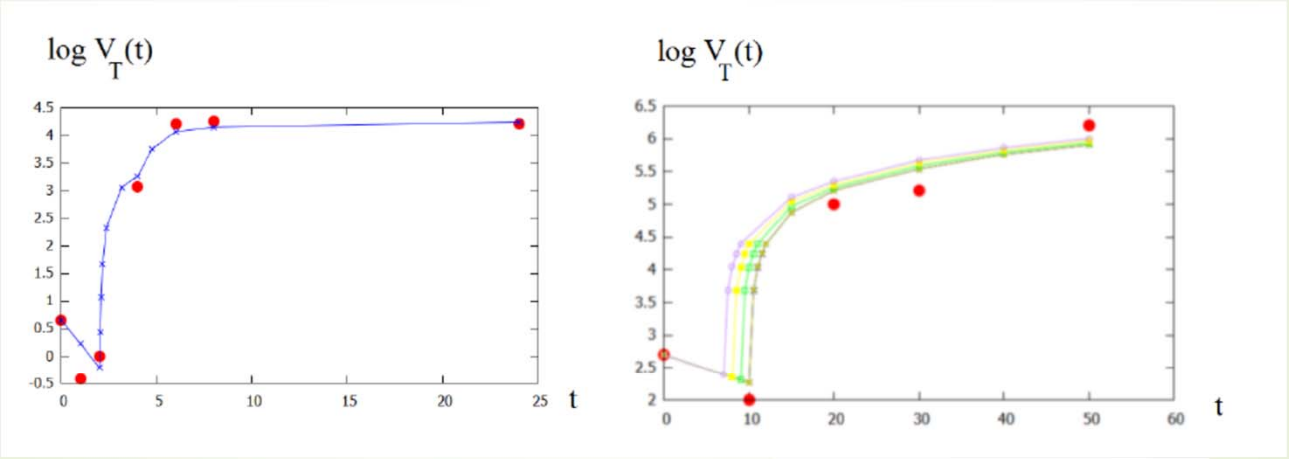

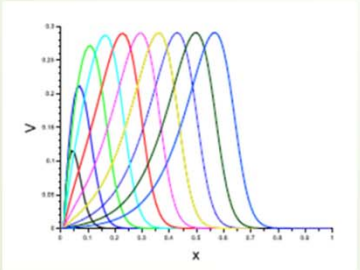

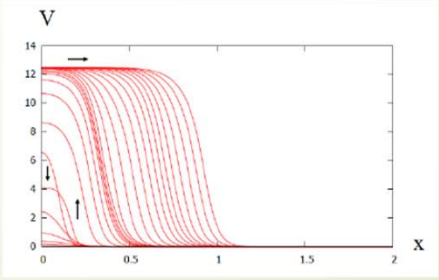

Distributed delay

$$\frac{\partial V}{\partial t} = D\frac{\partial^2 V}{\partial x^2} + \frac{b}{2h}\int_{t-\tau-h}^{t-\tau+h} I(x,s)ds - \sigma V$$

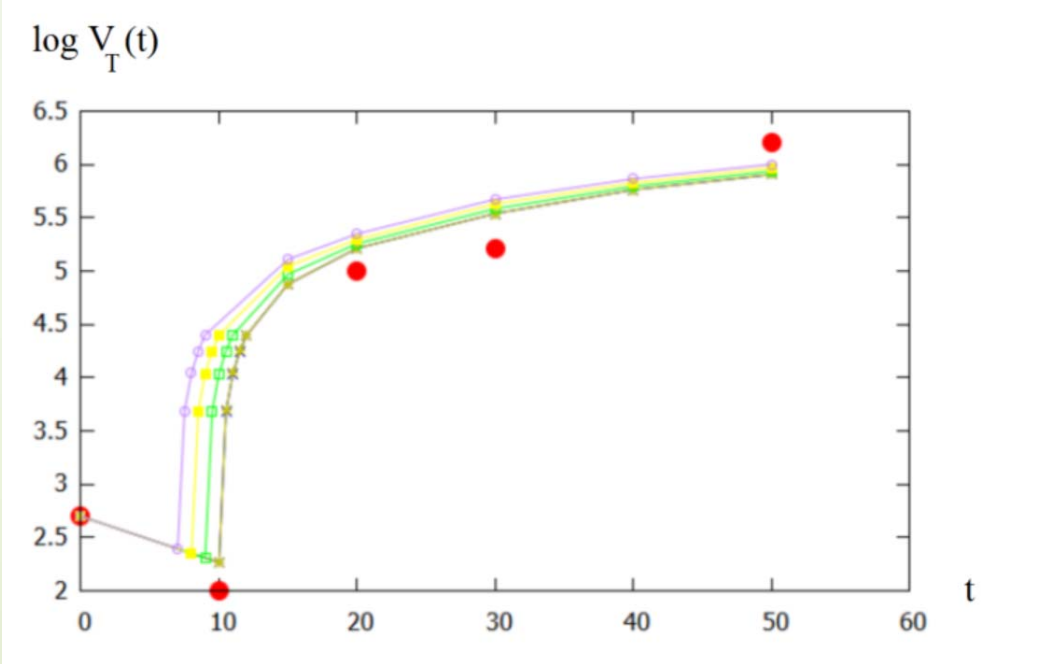

Viral infection and immune response

Models: ODE system and single equation

$$\frac{dv}{dt} = kv(1-v) - vc,$$

Virus

$$\frac{dc}{dt} = \phi(v_\tau)c(1-c) - \psi(v_\mu)c.$$

Immune cells

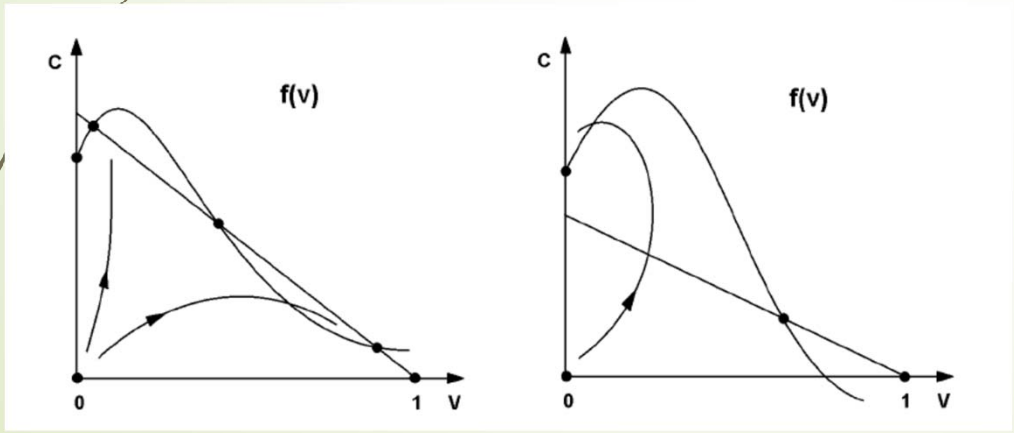

$c = f(v)$, where $f(v) = 1 - \frac{\psi(v)}{\phi(v)}$.

$$\frac{du}{dt} = ku(1-u-f(u_\tau))$$

Delay reaction-diffusion equation
for infection dynamics

N. Bessonov[1], G. Bocharov[2], T.M. Touaoula[3], S. Trofimchuk[4], V. Volpert[5,6,7]

Single delay equation: period doubling

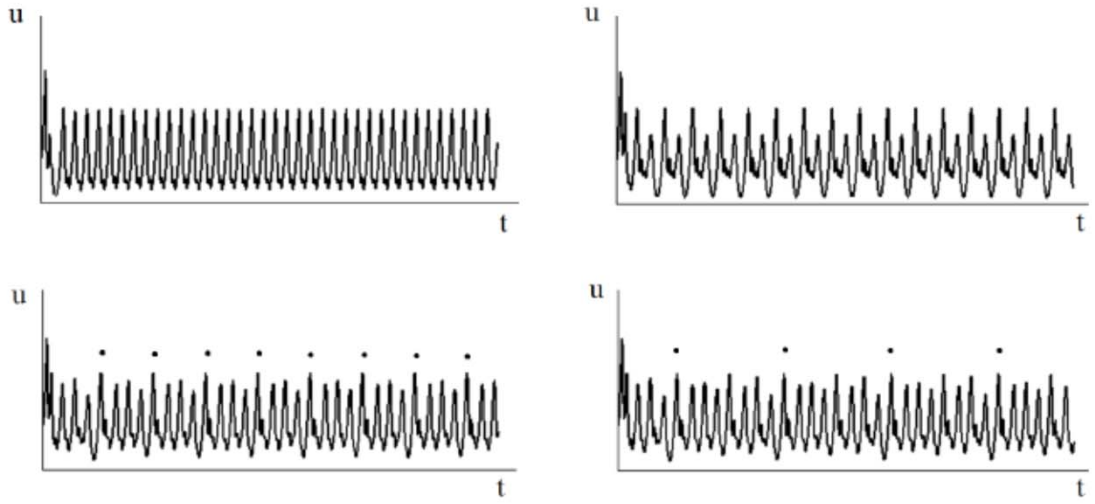

Figure 2: Period doubling bifurcations for the non-monotone function $f(u)$. Upper row: simple oscillations ($f_3 = 2.5$) and period 2 oscillations ($f_3 = 2$). Lower row: period 4 oscillations ($f_3 = 1.899$) and period 8 oscillations ($f_3 = 1.898$). The dots show the beginning of the periods. The values of parameters: $f_1 = 0, f_2 = 0.1, f_3$ varies, $u_1 = 0.1, u_2 = 0.3, u_3 = 0.5, \tau = 2$.

1D space equation

Spatiotemporal Dynamics of Virus Infection Spreading in Tissues

Gennady Bocharov[1,9,10]*, Andreas Meyerhans[1,2,3], Nickolai Bessonov[4], Sergei Trofimchuk[5], Vitaly Volpert[1,6,7,8]

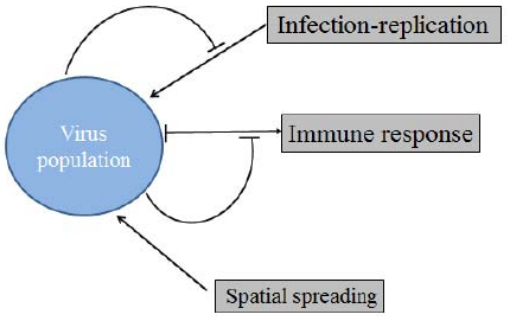

Immune response:

Time delay
Growth for small load
Decay for large load

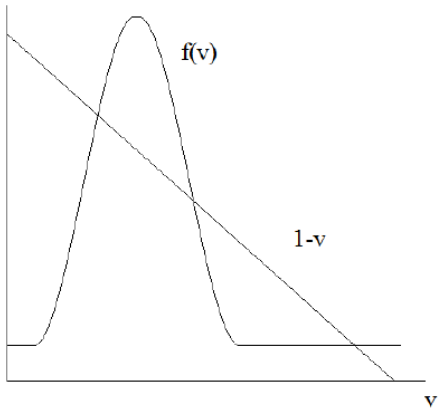

Local virus concentration in the tissue (lymph node, spleen)

$$\frac{\partial v}{\partial t} = D\frac{\partial^2 v}{\partial x^2} + kv(1-v) - f(v_\tau)v.$$

$$v = v(x,t),\ v_\tau = v(x,t-\tau)$$

Reaction-diffusion waves for the scalar equation

Monostable case: wave speeds greater than or equal to the minimal speed

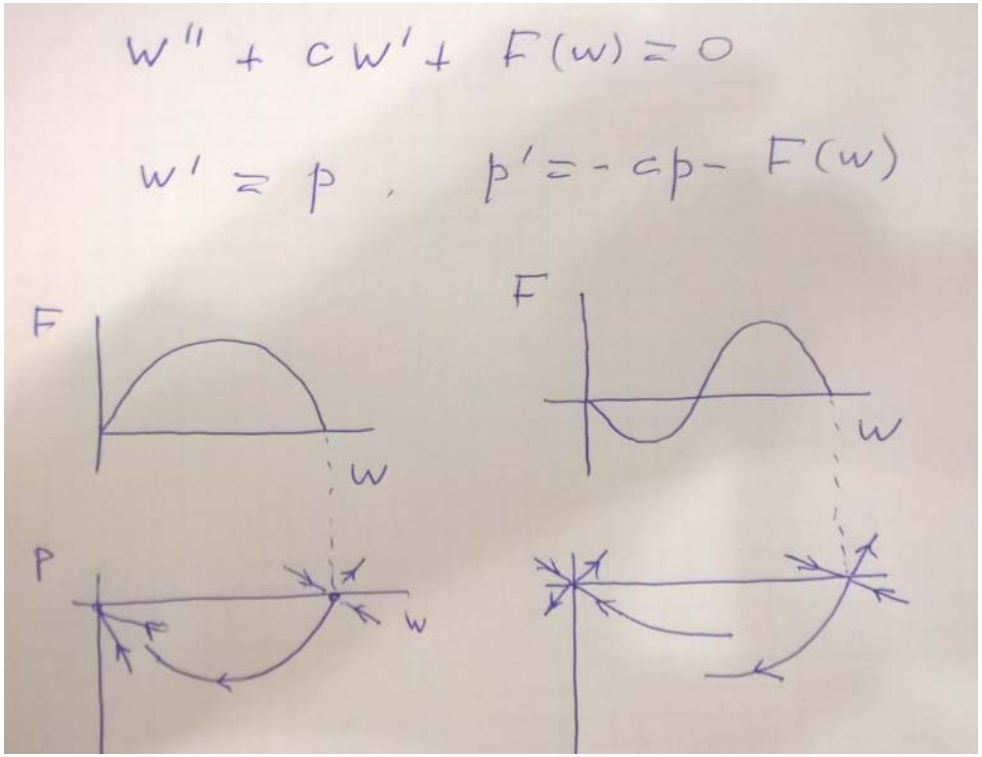

Bistable case: single wave speed

Systems of waves: bistable case

Scalar equation

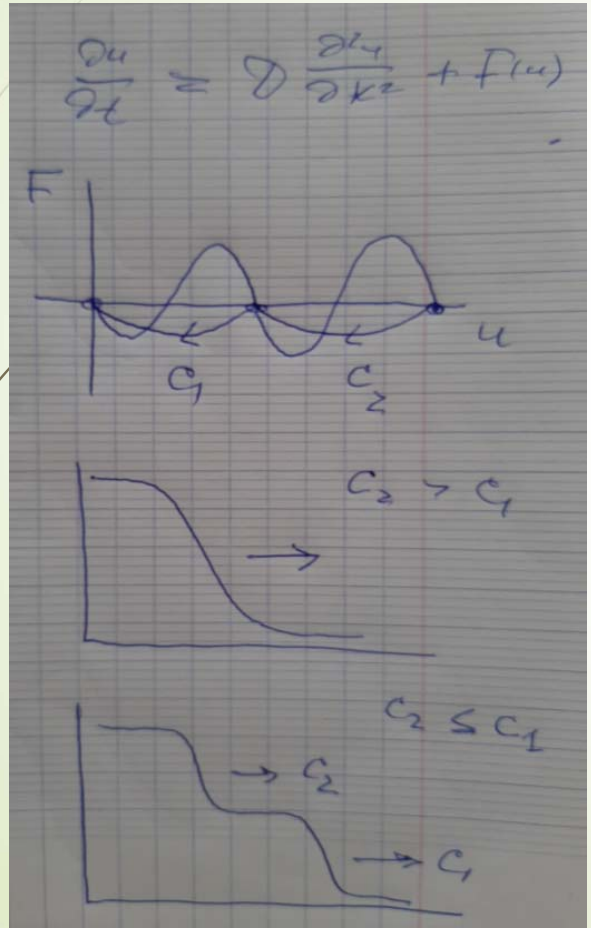

Monotone systems

$$\frac{\partial F_i}{\partial u_j} \geq 0, \quad i \neq j$$

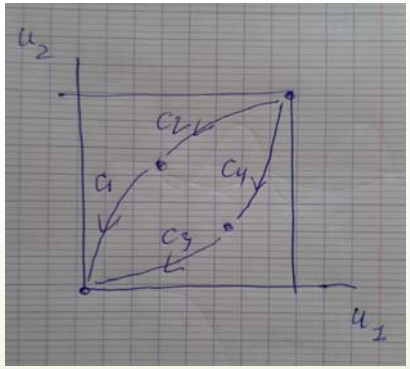

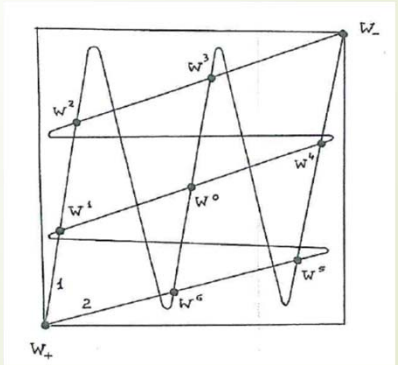

Systems of waves: monostable-bistable case

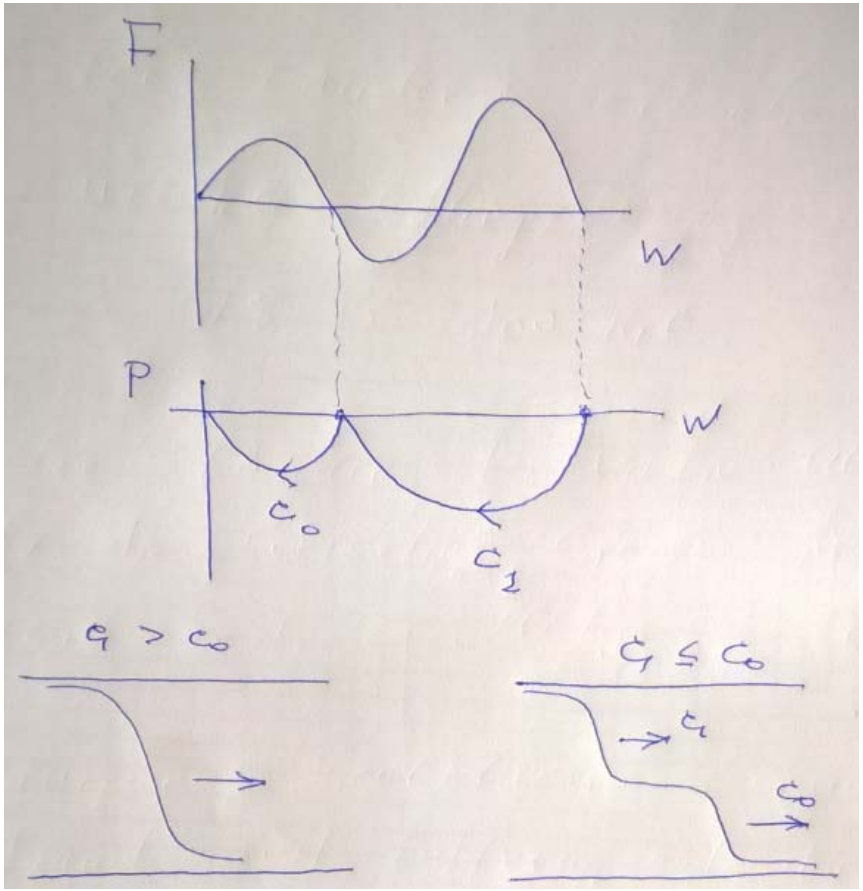

Virus spread

$$\frac{\partial v}{\partial t} = D\,\frac{\partial^2 v}{\partial x^2} + kv(1-v) - f(v)v.$$

$$F(v) = v\,(1 - v - f(v))\,.$$

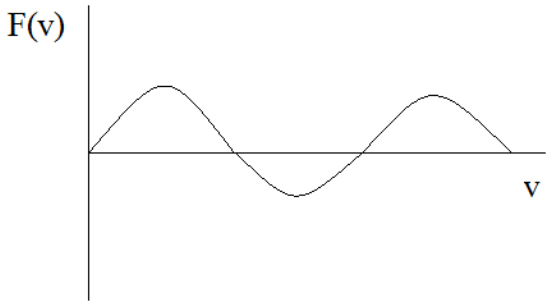

Three regimes of infection spreading:

Low dose
High dose
Low-High dose

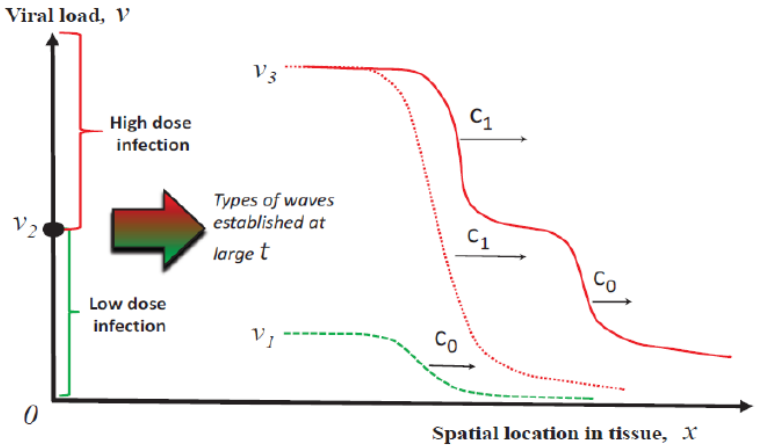

Evolution of quasi-species: genotype-dependent immune response

$$f(u) = (k_1(x)u + k_2)e^{-k_3 u}$$

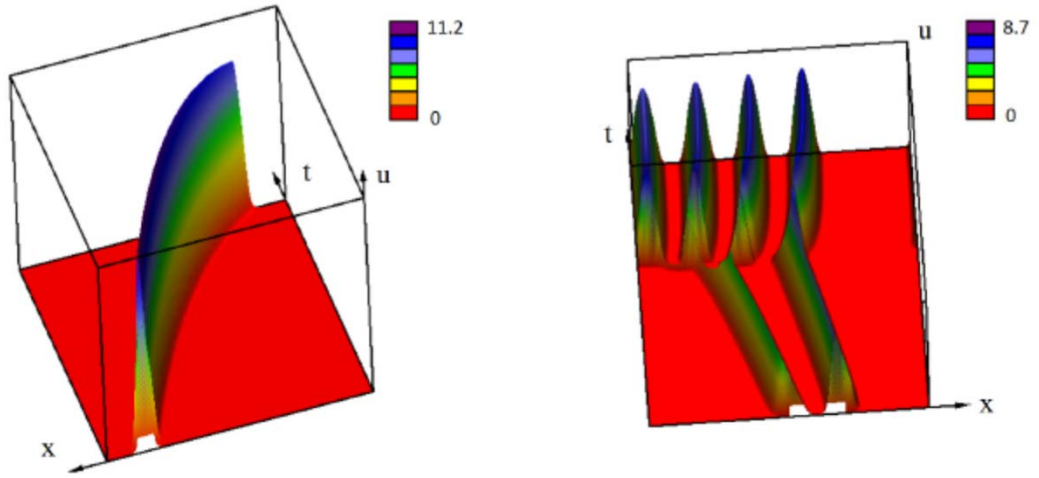

FIG. 5. *Virus dynamics in the case of a genotype-dependent immune response. The solution* $u(x,t)$ *is represented as a function of two variables. Left: a single virus strain evolves in the direction of a weaker immune response. Right: two virus strains evolve together while one of them splits into three other strains. The values of parameters are as follows:* $r = 1, q = 0.4, L = 1, D = 0.00005, N = 0.1$*;* $f(u) = (k_1(x)u + k_2)e^{-k_3 u}$*,* $k_1(x) = k_1^0 x$*;* $k_1^0 = 10, k_2 = 1.5, k_3 = 1$ *(left,* $k_1^0 = 0$ *during small initial period of time);* $k_1^0 = 5, k_2 = 1.5, k_3 = 2$ *(right).*

mathematics
MDPI
Article

Nonlocal Reaction–Diffusion Model of Viral Evolution: Emergence of Virus Strains

Nikolai Bessonov [1], Gennady Bocharov [2,3], Andreas Meyerhans [2,4,5], Vladimir Popov [6] and Vitaly Volpert [2,6,7,8,*]

Periodic structures and waves

$$\frac{\partial u}{\partial t} = D\frac{\partial^2 u}{\partial x^2} + ru(1 - qJ(u)) - f(u)u$$

$$J(u) = \int_{\infty}^{\infty} \phi(x - y)u(y, t)dy,$$

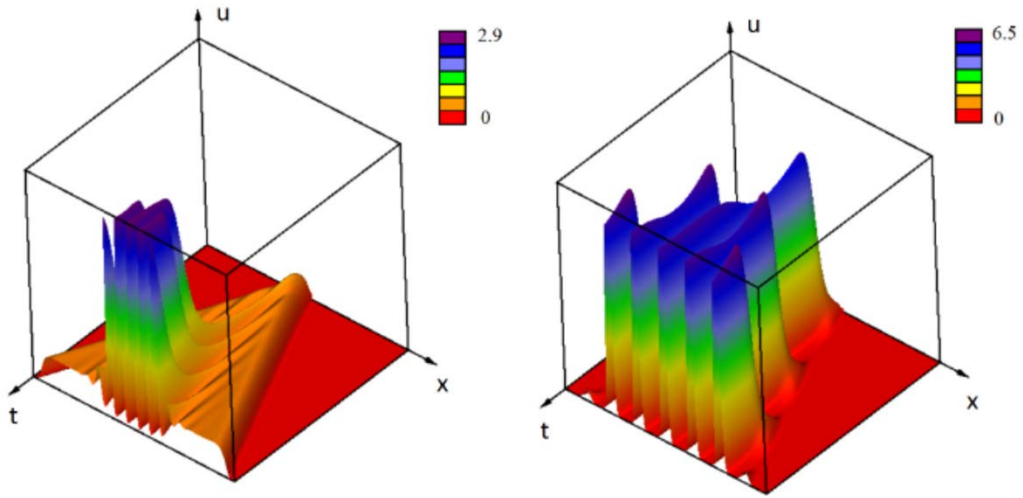

Figure 4. Numerical simulations of Equation (1) show the waves propagating from the center of the interval towards its boundaries in the monostable case. In the first monostable case (**left**) the periodic perturbation propagates slower than the $[u_+, u_-]$-wave, and the distance between them grows. In the second monostable case (**right**), the periodic perturbation propagates faster, it merges with the wave, and they form a single periodic wave. The values of parameters: $D = 10^{-5}, r = 1, q = 1, k_1 = 5, k_3 = 3$, $N = 0.035$ (**left**), $N = 0.1$ (**right**); $f(u) = k_1 u e^{-k_3 u}$, $\tau = 0$.

Nonlocl delay equation: wave propagation

$$\frac{\partial u}{\partial t} = D\frac{\partial^2 u}{\partial x^2} + ru(1 - qJ(u)) - uf(S(u_\tau))$$

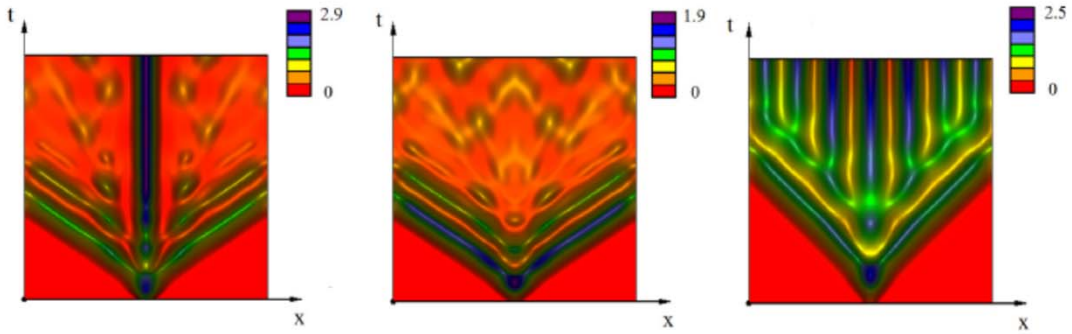

Figure 8. Numerical simulations of Equation (1). Virus evolution with time delay in the term describing the immune response represented as level lines of the solution $u(x,t)$ on the (x,t)-plane. Different regimes coexist for the same values of parameters depending on the initial conditions, with high initial viral load (**left**) and low initial viral load (**middle**). Values of parameters: $D = 10^{-4}, r = 1, q = 1, N = 0.1, f(u) = k_1 e^{-k_3 u}, k_1 = 8, k_3 = 3, t = 80$ (**left** and **middle**), $k_3 = 6, t = 50$ (**right**); the maximum of the initial condition 0.9 (**left**), 0.1 (**middle** and **right**).

Part 2c. Brain modelling:

normal functioning, disorders, stimulation

Connectome

Neurorehabil Neural Repair. 2016 March ; 30(3): 266–279. doi:10.1177/1545968315593808.

Success of anomia treatment in aphasia is associated with preserved architecture of global and left temporal lobe structural networks

Leonardo Bonilha, MD PhD[1], Ezequiel Gleichgerrcht, MD[1], Travis Nesland[1], Chris Rorden, PhD[2], and Julius Fridriksson, PhD[3]

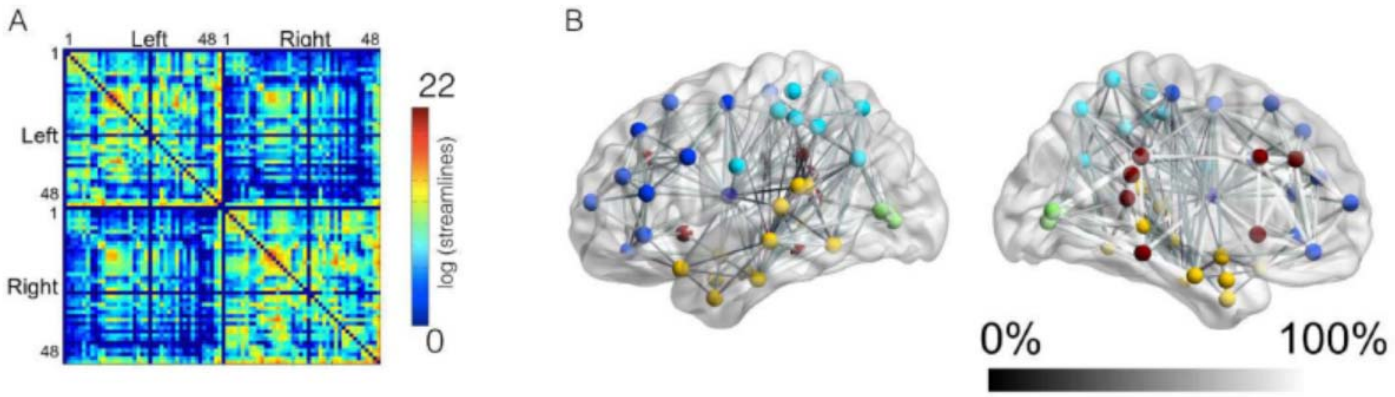

Figure 4.

This diagram demonstrates the average connectome in panel A, with axis numbers corresponding to BAs. The scale bar demonstrates the link-wise strength, which corresponds to the log of the number of streamlines connecting the ROIs (corrected based on ROI volume and distance travelled by the streamlines). Panel B demonstrates the link-wise asymmetry in connectivity, illustrating how often links in the left hemisphere were present, in comparison with the homologous right hemisphere links that were present in 100% of subjects. A sphere in its center of mass illustrates the location of each BA ROI; straight lines connecting the nodes demonstrate links; the shade of gray of each link corresponds to its frequency of observation in comparison with the right hemisphere. The colors of the nodes illustrate their anatomical locations (light blue – parietal and inferior frontal; dark blue – frontal; yellow – temporal; dark red – pericingulate regions and insula, green – occipital).

Functional brain networks

Dynamic reorganization of functional brain networks during picture naming

Mahmoud Hassan [a,b,], Pascal Benquet [a,b], Arnaud Biraben [a,b,c], Claude Berrou [d,e], Olivier Dufor [d,e] and Fabrice Wendling [a,b]*

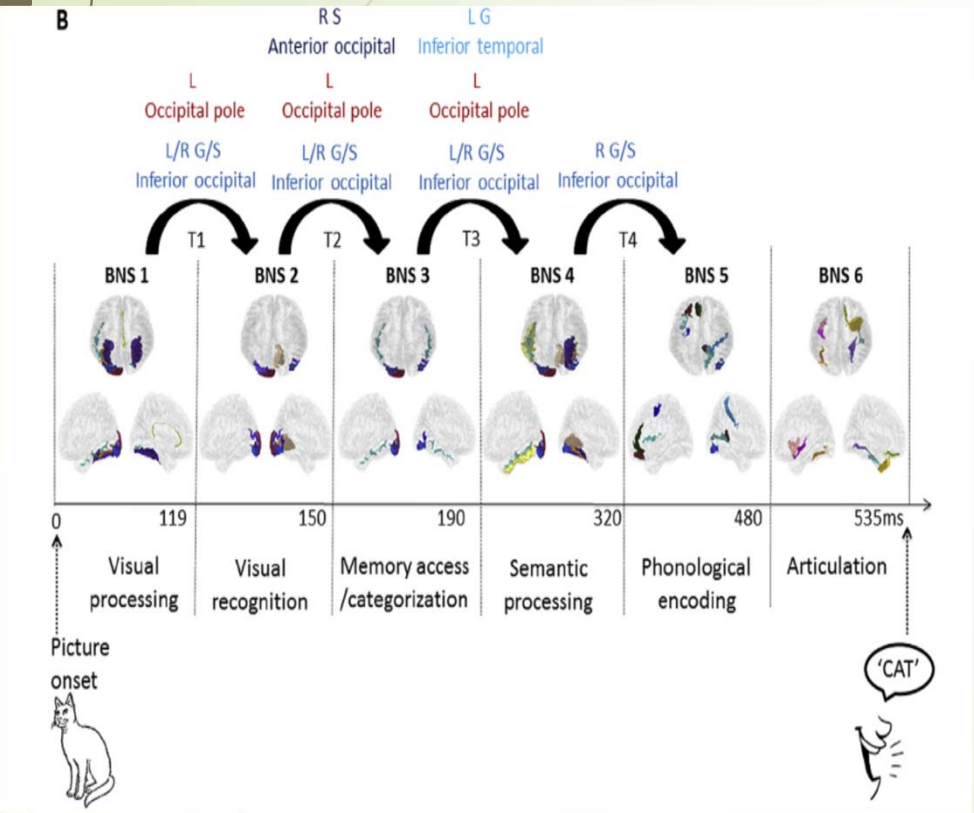

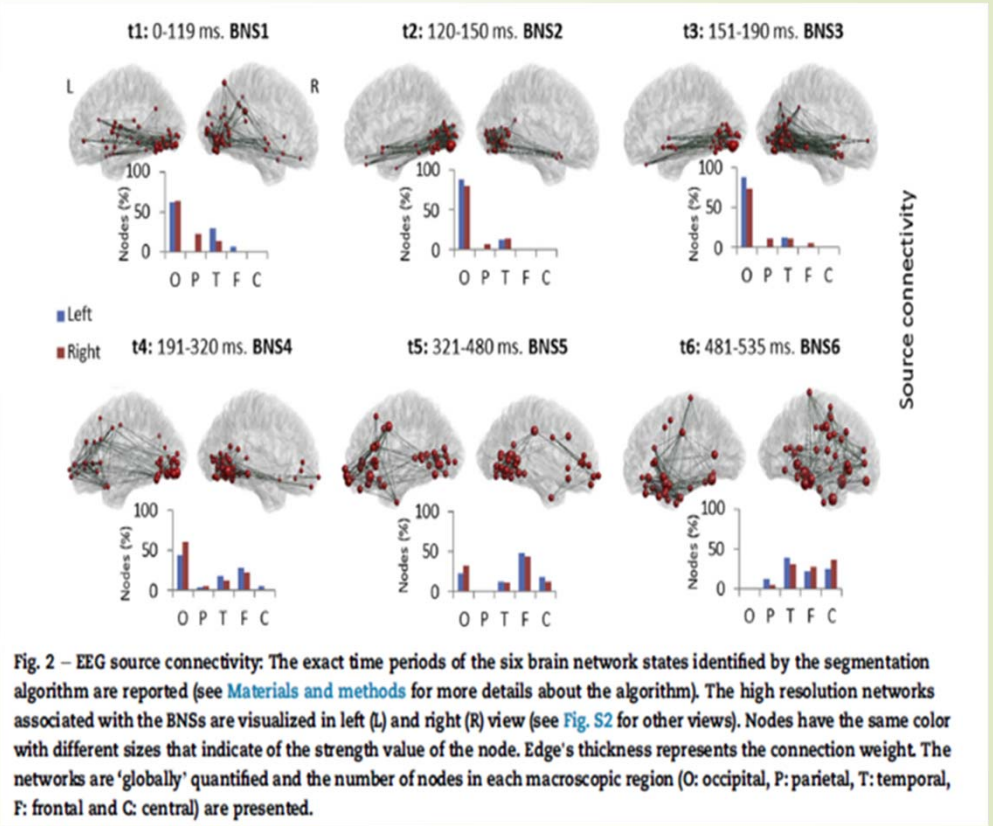

Fig. 2 – EEG source connectivity: The exact time periods of the six brain network states identified by the segmentation algorithm are reported (see Materials and methods for more details about the algorithm). The high resolution networks associated with the BNSs are visualized in left (L) and right (R) view (see Fig. S2 for other views). Nodes have the same color with different sizes that indicate of the strength value of the node. Edge's thickness represents the connection weight. The networks are 'globally' quantified and the number of nodes in each macroscopic region (O: occipital, P: parietal, T: temporal, F: frontal and C: central) are presented.

Brain waves (EEG data)

eLIFE elifesciences.org

RESEARCH ARTICLE

Electrocorticographic dissociation of alpha and beta rhythmic activity in the human sensorimotor system

Arjen Stolk[1,2]*, Loek Brinkman[3], Mariska J Vansteensel[3], Erik Aarnoutse[3], Frans SS Leijten[3], Chris H Dijkerman[4], Robert T Knight[1], Floris P de Lange[2], Ivan Toni[2]

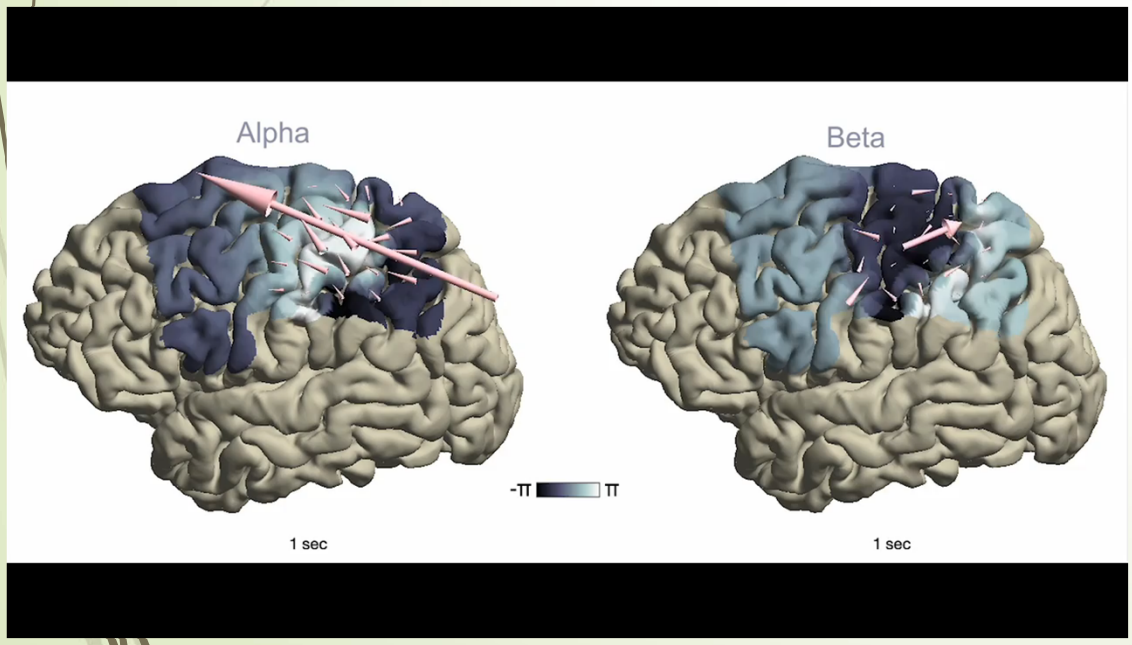

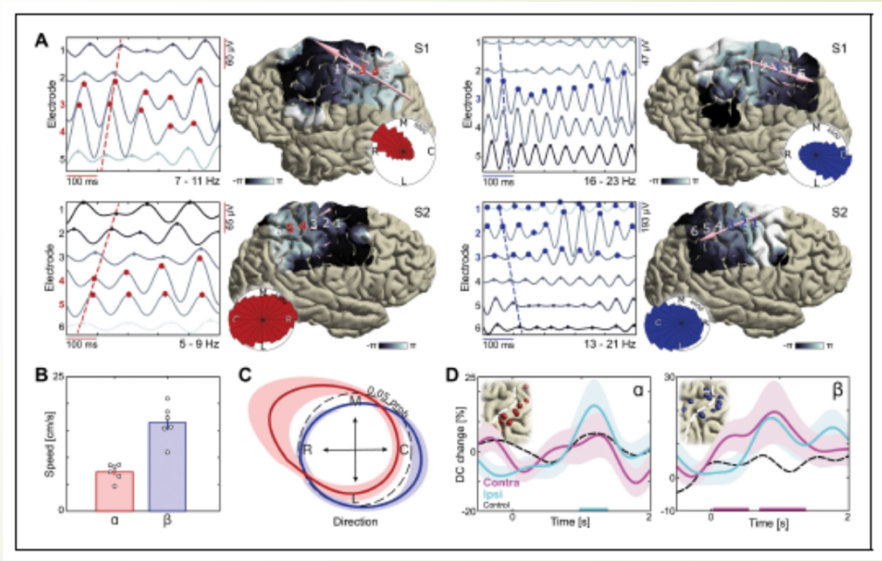

Rotating waves

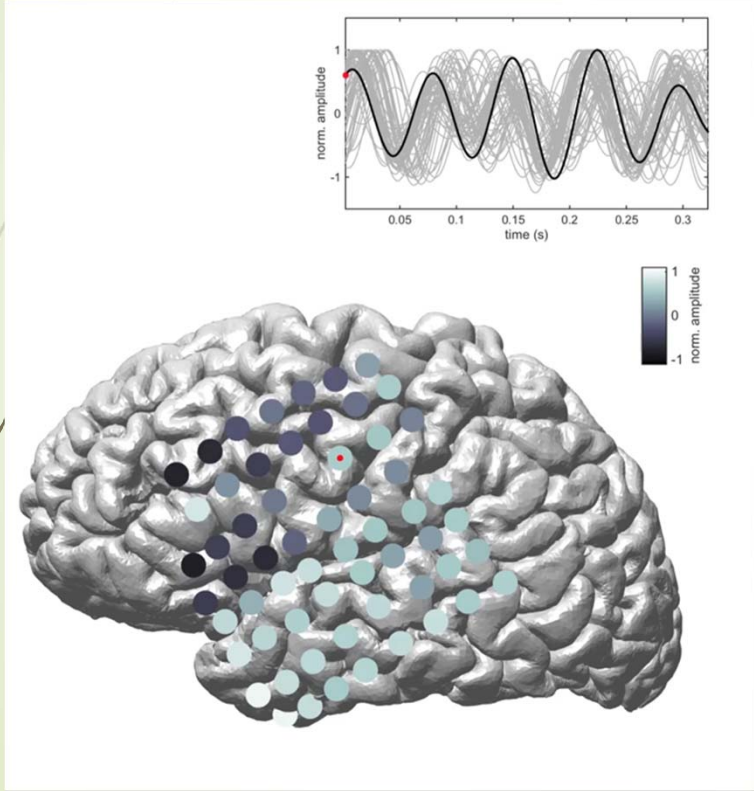

eLIFE
elifesciences.org
SHORT REPORT

Rotating waves during human sleep spindles organize global patterns of activity that repeat precisely through the night

Lyle Muller[1], Giovanni Piantoni[2], Dominik Koller[1], Sydney S Cash[2], Eric Halgren[3,4], Terrence J Sejnowski[1]*

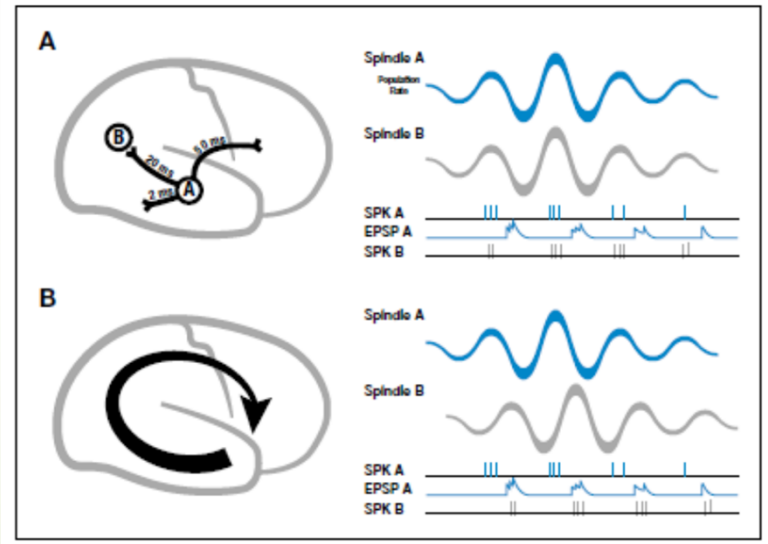

EEG waves

Plane waves

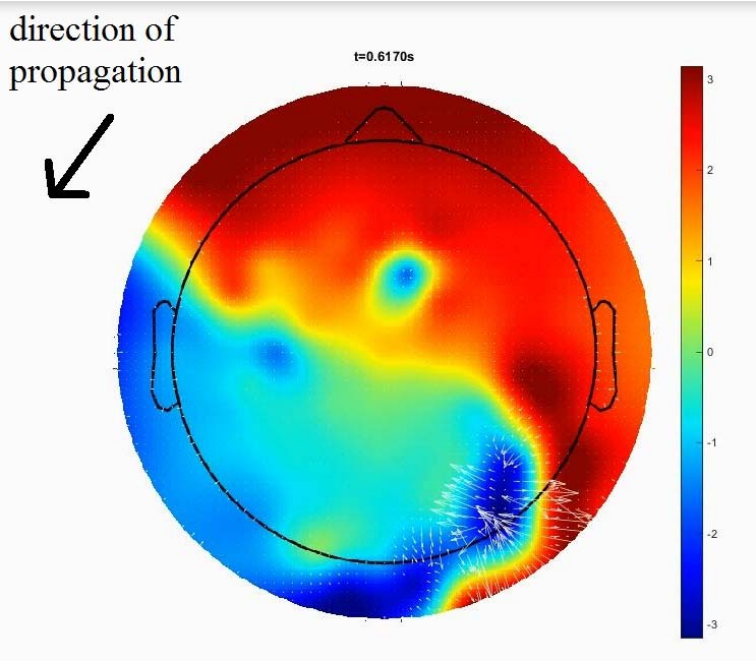

Rotating waves

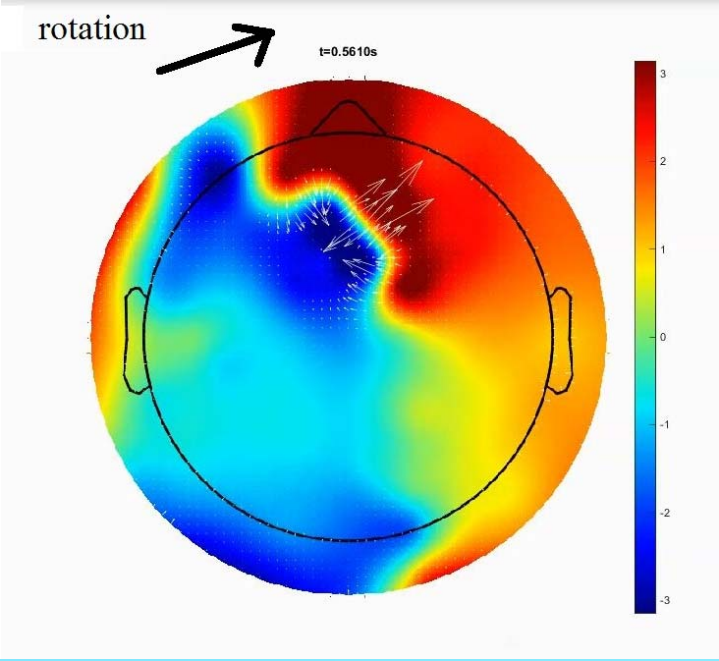

Neural field models

Two equations with time delay

$$\tau\frac{\partial u}{\partial t} = \int_{-\infty}^{\infty} (P_{11}(x-y)\psi_1(u(y,t-d)) - P_{12}(x-y)\psi_2(v(y,t-d))\,dy - u$$

$$\tau\frac{\partial v}{\partial t} = \int_{-\infty}^{\infty} (P_{21}(x-y)\psi_1(u(y,t-d)) - P_{22}(x-y)\psi_2(v(y,t-d))\,dy - v$$

D.J. Pinto, G.B. Ermentrout. Spatially structured activity in synapticalaly coupled neuronal networks: II. Lateral inhibition and standing pulses. SIAM J. Appl. Math., 62 (2001), No. 1, 226-243.

Distributed speed and delay

$$L\left(\frac{\partial u}{\partial t}\right) = \alpha\int_0^{\infty} g(v)\int_{-\infty}^{\infty} K(z)S(u(x+z,t-|z|/v))dzdv+$$
$$\beta\int_0^{\infty} f(\tau)\int_{-\infty}^{\infty} F(z)S(u(x+z,t-\tau))dzd\tau,$$

$$u(x,t) = \int_{-\infty}^{\infty} w(x-y)dy\int_{-\infty}^{t} \eta(t-s)f(u(y,s-|x-y|/v))ds.$$

F.M. Atay, A. Hutt. Neural Fields with Distributed Transmission Speeds and Long-Range Feedback Delays. SIAM J. Applied Dynamical Systems, 5 (2006), No. 4, 670-698.

N.A. Venkov, S. Coombes, P.C. Matthews. Dynamic instabilities in scalar neural field equations with space-dependent delays. Physica D, 232 (2007), 1-15.

Linear adaptation

$$\tau\frac{\partial u}{\partial t} = -u - \beta v + \int_D w(x-y)F(u(y,t))dy,$$

$$\frac{1}{\alpha}\frac{\partial v}{\partial t} = u - v,$$

G. Bard Ermentrout, Stefanos E. Folias, and Zachary P. Kilpatrick Spatiotemporal Pattern Formation in Neural Fields with Linear Adaptation, 119-151. In: S. Coombes et al. (eds.), Neural Fields, Springer-Verlag Berlin Heidelberg, 2014,

Refractoriness

$$\frac{1}{r}\frac{\partial u}{\partial t} = -u + \left(1 - \int_{t-1}^{t} u(x,s)ds\right) f(w\otimes u).$$

H.G.E. Meijer, S. Coombes. Travelling waves in a neural field model with refractoriness. J. Math. Biol., 68 (2014), 1249-1268.

Stability analysis – Pattern formation

$$\frac{\partial u}{\partial t} = d\,\frac{\partial^2 u}{\partial x^2} + ku\left(1 - \int_{-\infty}^{\infty} \phi(x-y)u(y,t)dy\right)$$

Homogeneous in space stationary solutions: $u = 0,\ u = 1$

Spectrum of the linearized operator

$$du'' - \sigma \int_{-\infty}^{\infty} \phi(x-y)u(y)dy = \lambda u$$

Fourier transform

$$-\lambda = d\xi^2 + \frac{\sigma}{\xi N}\,\sin(\xi N)$$

Instability condition: $d/(\sigma N^2) < \text{const}$

Bifurcation of periodic structures

$$\frac{\partial u}{\partial t} = d\,\frac{\partial^2 u}{\partial x^2} + ku\left(1 - \int_{-\infty}^{\infty} \phi(x-y)u(y,t)dy\right)$$

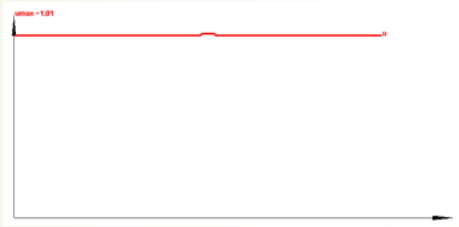

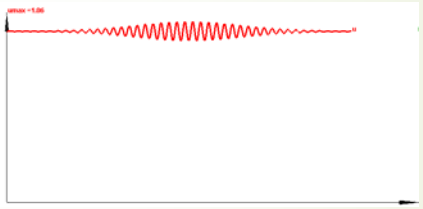

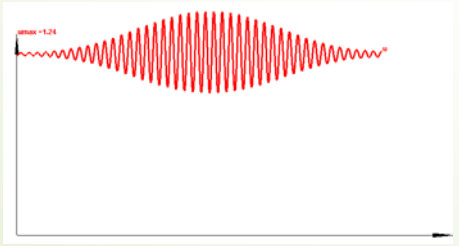

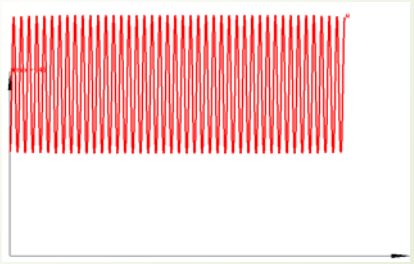

Nonlocal consumption: periodic wave

$$\frac{\partial u}{\partial t} = d\,\frac{\partial^2 u}{\partial x^2} + ku\left(1 - \int_{-\infty}^{\infty} \phi(x-y)u(y,t)dy\right)$$

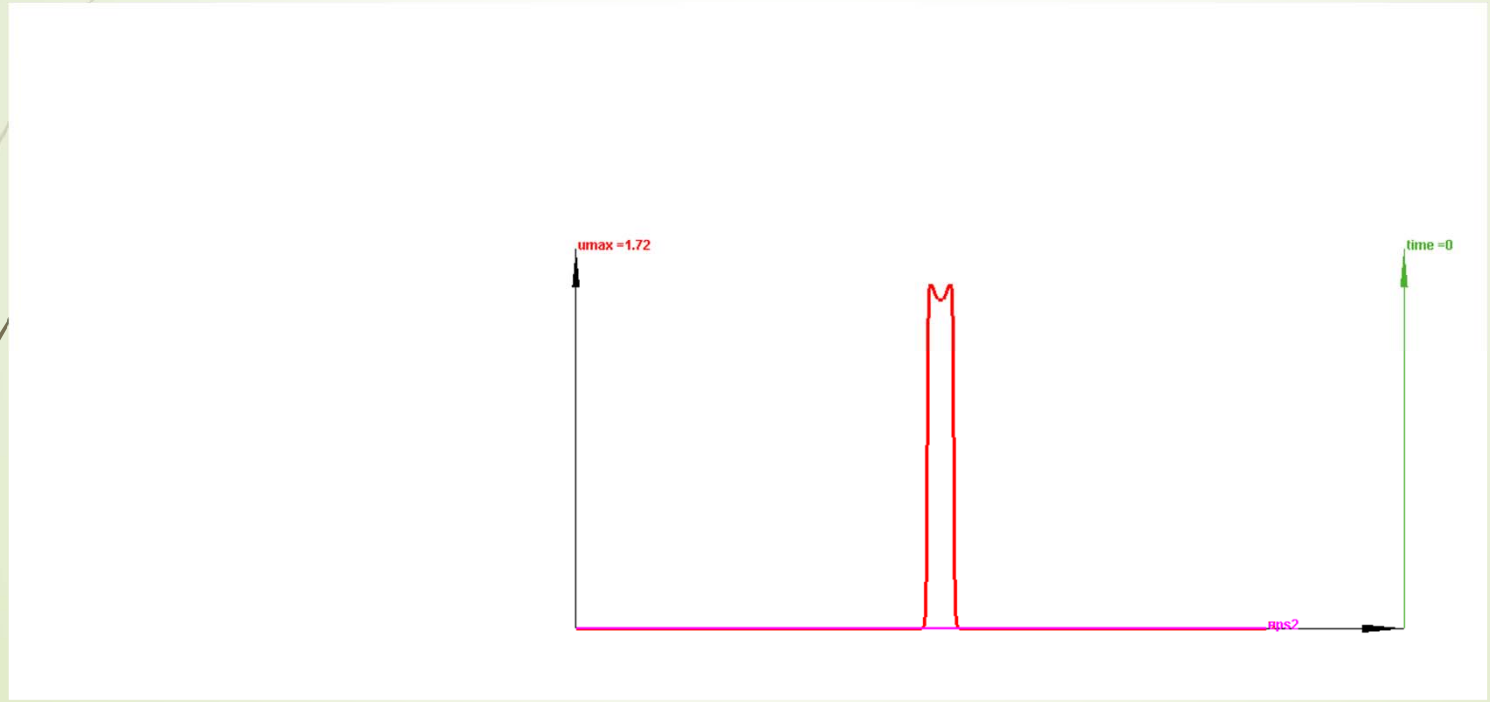

Model with inhibition

$$\frac{\partial u}{\partial t} = D\frac{\partial^2 u}{\partial x^2} + \int_{-\infty}^{\infty} (\phi_a(x-y)S_a(u(y,t)) - \phi_i(x-y)S_i(u(y,t)))\,dy - \sigma u$$

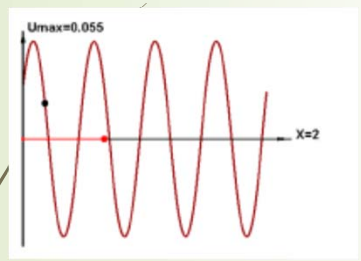

Stationary structures
Periodic waves two types
Aperiodic waves

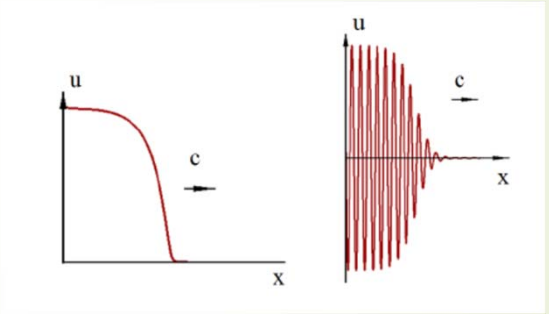

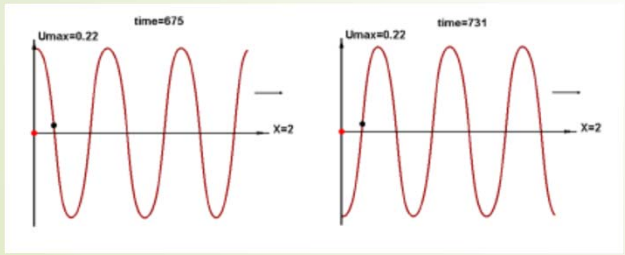

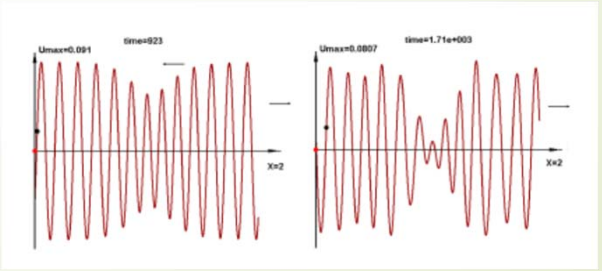

Wave propagation: normal tissue

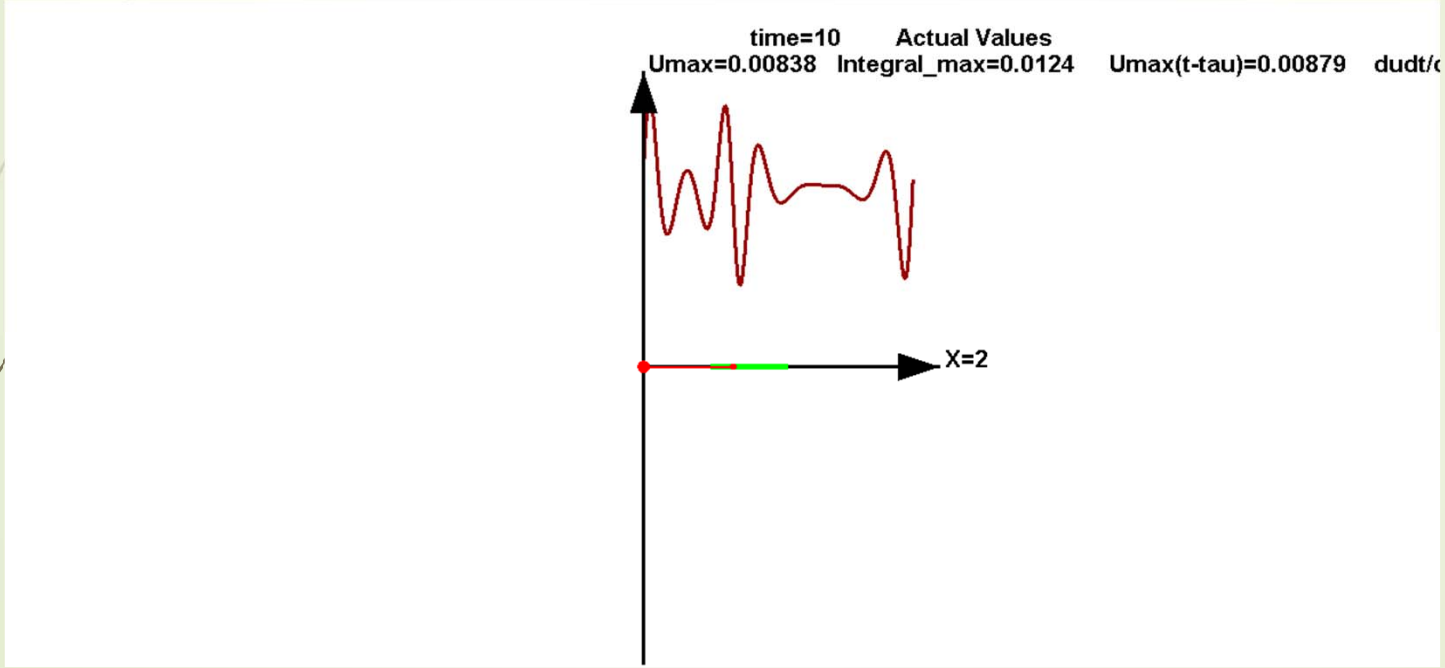

Conclusions

- Physiological systems are often characterized by the presence of a stable equilibrium (ex: disease-free, quiescent state)
- Activation of physiological processes can lead to the emergence of other stable equilibria (ex: endemic) or other spatiotemporal structures (excitable media – brain, heart)
- Transition between the equilibria (ex: disease development) can be described by reaction-diffusion waves